

Spatiotemporal chaos in disordered nonlinear lattices

Haris Skokos

**Department of Mathematics and Applied Mathematics
University of Cape Town
Cape Town, South Africa**

E-mail: haris.skokos@uct.ac.za

URL: http://math_research.uct.ac.za/~hskokos/

**Scientific Workshop: 30 years MPI-PKS
7 September 2023, Dresden, Germany**

All started back in 2008



University of Cape Town (UCT)



University of Cape Town (UCT)



Cape Town



Outline

- **Brief overview of the dynamics of 1D Disordered lattices:**
 - ✓ **The quartic disordered Klein-Gordon (DKG) model**
 - ✓ **The disordered discrete nonlinear Schrödinger equation (DDNLS)**
 - ✓ **Different dynamical regimes**
- **Symplectic Integrators – Tangent Map Method**
- **Numerical investigation of chaos**
 - ✓ **Maximum Lyapunov Exponent (MLE): strength of chaos**
 - ✓ **Deviation Vector Distributions (DVDs): mechanisms of chaotic spreading**
 - ✓ **Frequency Map Analysis (FMA): characteristics of spatiotemporal evolution of chaos**
 - ✓ **Generalized Alignment Index (GALI): localized vs. spreading chaos**
- **Chaotic behavior of the DKG and DDNLS models in 2 spatial dimensions**

The 1D disordered Klein – Gordon model (1D DKG)

$$H_{1K} = \sum_{l=1}^N \frac{p_l^2}{2} + \frac{\tilde{\varepsilon}_l}{2} u_l^2 + \frac{1}{4} u_l^4 + \frac{1}{2W} (u_{l+1} - u_l)^2$$

with **fixed boundary conditions** $u_0=p_0=u_{N+1}=p_{N+1}=0$. Typically $N=1000$.

Parameters: W and the total energy E . $\tilde{\varepsilon}_l$ chosen uniformly from $\left[\frac{1}{2}, \frac{3}{2} \right]$.

Linear case (neglecting the term $u_l^4/4$)

Ansatz: $u_l = A_l \exp(i\omega t)$. Normal modes (NMs) $A_{\nu,l}$ - Eigenvalue problem:

$$\lambda A_l = \varepsilon_l A_l - (A_{l+1} + A_{l-1}) \text{ with } \lambda = W\omega^2 - W - 2, \quad \varepsilon_l = W(\tilde{\varepsilon}_l - 1)$$

The 1D disordered discrete nonlinear Schrödinger equation (1D DDNLS)

We also consider the system:

$$H_{1D} = \sum_{l=1}^N \varepsilon_l |\psi_l|^2 + \frac{\beta}{2} |\psi_l|^4 - (\psi_{l+1} \psi_l^* + \psi_{l+1}^* \psi_l)$$

where ε_l chosen uniformly from $\left[-\frac{W}{2}, \frac{W}{2} \right]$ and β is the nonlinear parameter.

Conserved quantities: The energy and the norm $S = \sum_l |\psi_l|^2$ of the wave packet.

Distribution characterization (1D case)

We consider normalized **energy distributions** $\xi_l \equiv \frac{E_l}{\sum_m E_m}$

with $E_l = \frac{p_l^2}{2} + \frac{\tilde{\varepsilon}_l}{2} u_l^2 + \frac{1}{4} u_l^4 + \frac{1}{4W} (u_{l+1} - u_l)^2$ for the DKG model,

and **norm distributions** $\xi_l \equiv \frac{|\psi_l|^2}{\sum_m |\psi_m|^2}$ for the DDNLS system.

Second moment: $m_2 = \sum_{l=1}^N (l - \bar{l})^2 \xi_l$ with $\bar{l} = \sum_{l=1}^N l \xi_l$

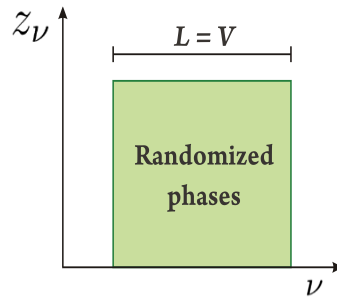
Participation number: $P = \frac{1}{\sum_{l=1}^N \xi_l^2}$

measures the number of stronger excited sites in ξ_l .

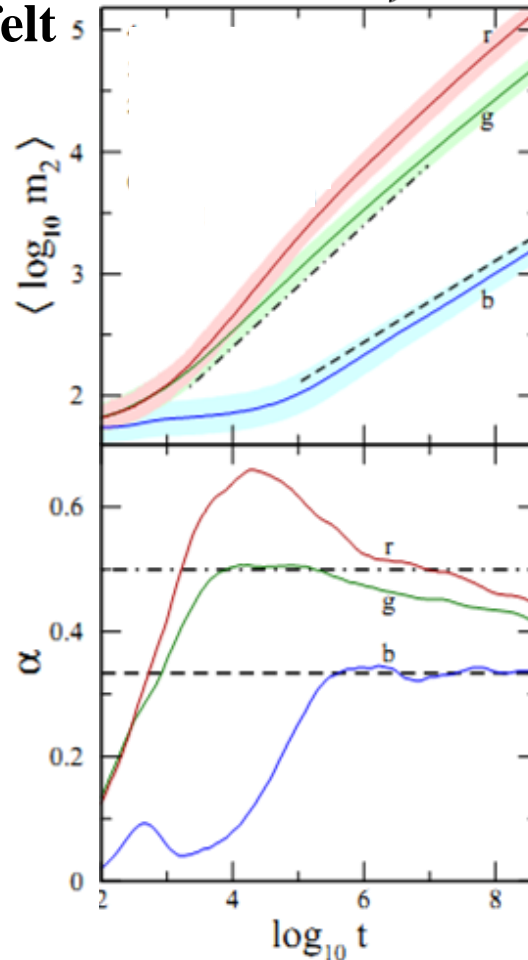
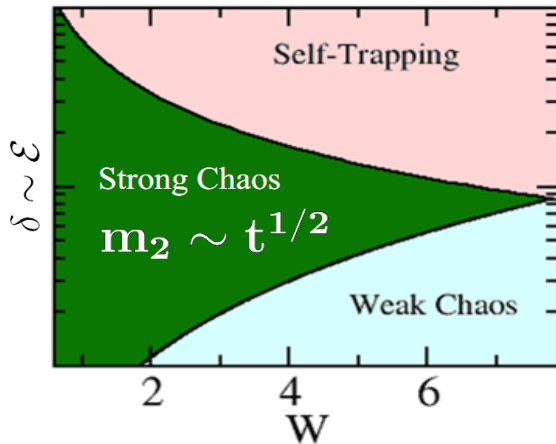
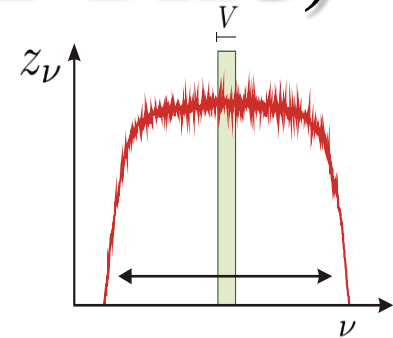
Single site $P=1$. Equipartition of energy $P=N$.

Strong and weak chaos regimes (1D DKG)

We consider **compact initial wave packets of width L**
 [Flach et al. PRL (2009) – S. et al PRE (2009) – Lapyteva et al., EPL (2010) – Bodyfelt et al., PRE (2011)]



Time evolution



$H = 0.01, 0.2, 0.75$

$W = 4$

Average over 1000 realizations!

$$\alpha(\log t) = \frac{d\langle \log m_2 \rangle}{d \log t}$$

Maximum Lyapunov Exponent (MLE)

Chaos: sensitive dependence on initial conditions.

Roughly speaking, the MLE of a given orbit characterizes the **mean exponential rate of divergence** of trajectories surrounding it.

Consider an orbit in the $2N$ -dimensional phase space with **initial condition $\mathbf{x}(0)$** and **an initial deviation vector (small perturbation) from it $\mathbf{v}(0)$** .

Then the mean exponential rate of divergence is:

$$\text{MLE} = \lambda_1 = \lim_{t \rightarrow \infty} \Lambda(t) = \lim_{t \rightarrow \infty} \frac{1}{t} \ln \frac{\|\mathbf{v}(t)\|}{\|\mathbf{v}(0)\|}$$

$\lambda_1 = 0 \rightarrow$ Regular motion ($\Lambda \propto t^{-1}$)

$\lambda_1 > 0 \rightarrow$ Chaotic motion

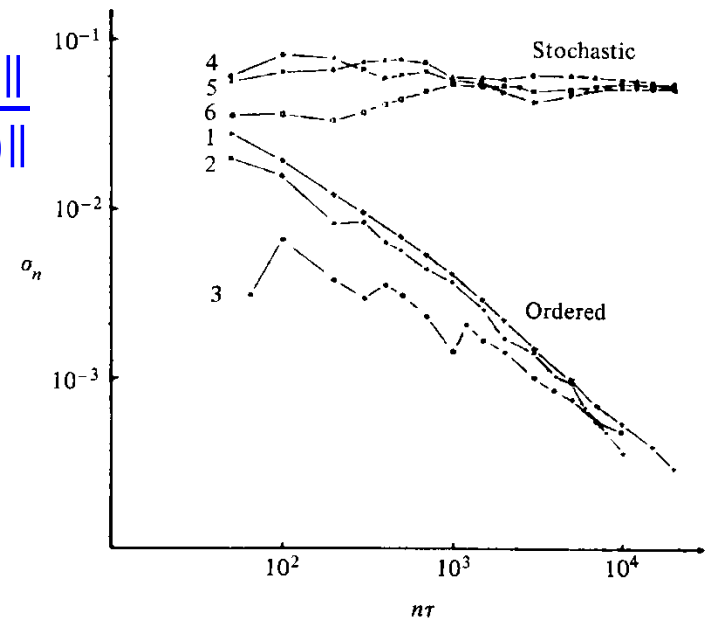


Figure 5.7. Behavior of σ_n at the intermediate energy $E = 0.125$ for initial points taken in the ordered (curves 1–3) or stochastic (curves 4–6) regions (after Benettin *et al.*, 1976).

Symplectic integration

We apply **the 2-part splitting integrator ABA864** [Blanes et al., Appl. Num. Math. (2013) – Senyange & S., EPJ ST (2018)] to the DKG model:

$$H_{IK} = \sum_{l=1}^N \left(\frac{p_l^2}{2} + \frac{\tilde{\varepsilon}_l}{2} u_l^2 + \frac{1}{4} u_l^4 + \frac{1}{2W} (u_{l+1} - u_l)^2 \right)$$

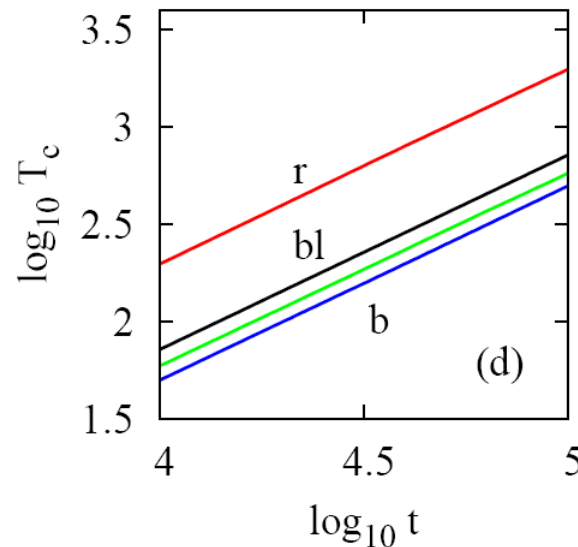
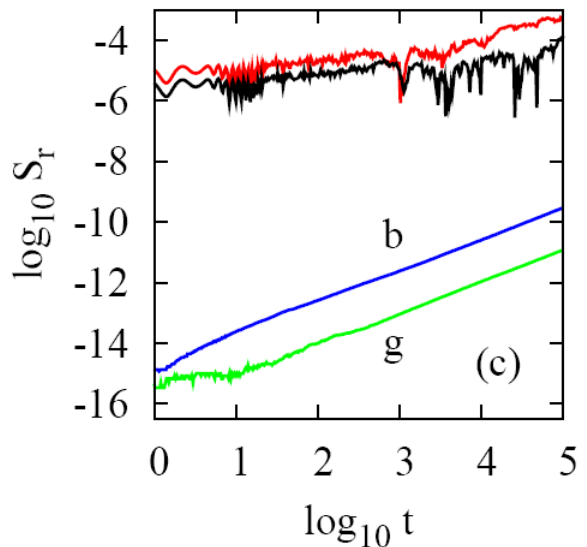
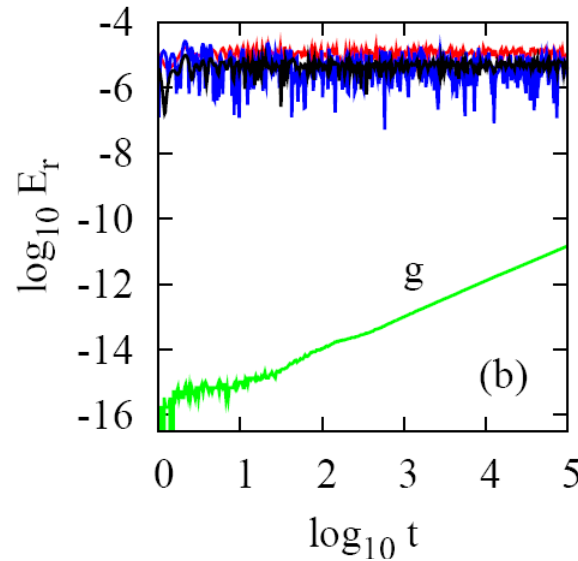
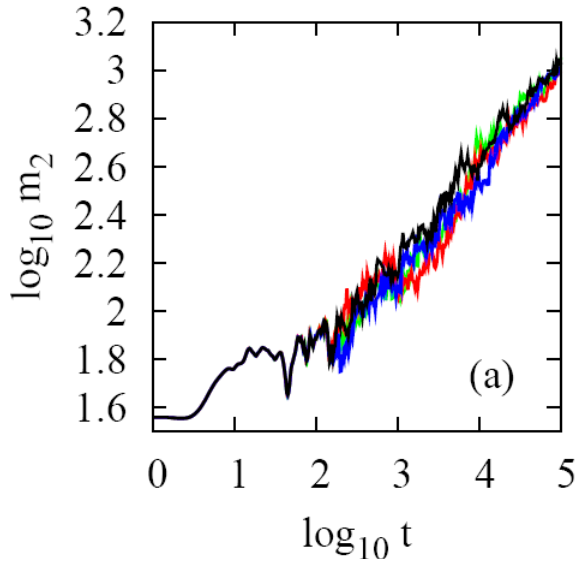
and **the 3-part splitting integrator ABC⁶_[SS]** [S. et al., Phys. Let. A (2014) – Gerlach et al., EPJ ST (2016) – Danieli et al., MinE (2019)] to the DDNLS system:

$$H_{ID} = \sum_l \varepsilon_l |\psi_l|^2 + \frac{\beta}{2} |\psi_l|^4 - (\psi_{l+1} \psi_l^* + \psi_{l+1}^* \psi_l), \quad \psi_l = \frac{1}{\sqrt{2}} (u_l + ip_l)$$

$$H_{ID} = \sum_l \left(\frac{\varepsilon_l}{2} (u_l^2 + p_l^2) + \frac{\beta}{8} (u_l^2 + p_l^2)^2 - u_n u_{n+1} - p_n p_{n+1} \right)$$

By using the so-called **Tangent Map method** we extend these symplectic integration schemes in order to integrate simultaneously the variational equations [S. & Gerlach, PRE (2010) – Gerlach & S., Discr. Cont. Dyn. Sys. (2011) – Gerlach et al., IJBC (2012)].

2nd order integrators: Numerical results (1D DDNLS)



ABC² $\tau=0.005$

SS² $\tau=0.02$

DOP853 $\delta=10^{-16}$

SIFT² $\tau=0.05$

E_r : relative energy error

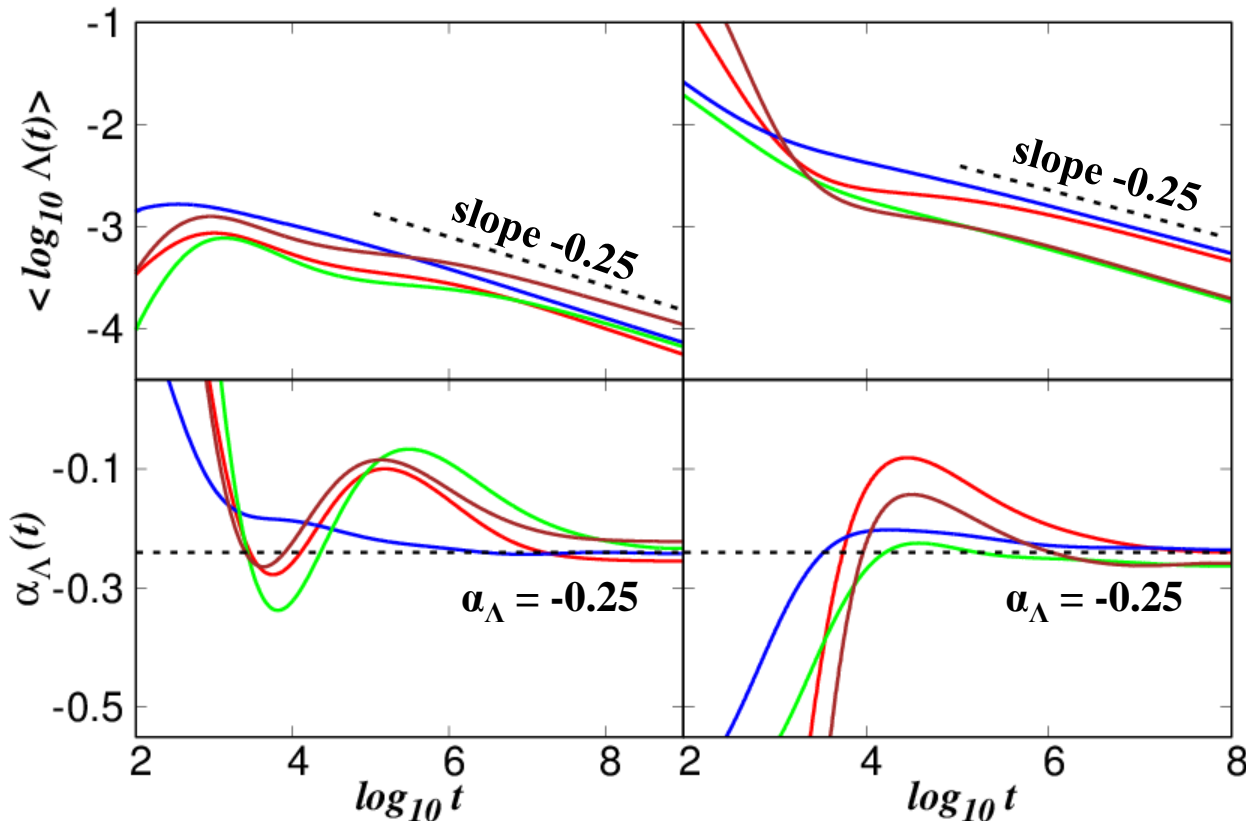
S_r : relative norm error

T_c : CPU time (sec)

S. et al., Phys. Lett. A (2014)

Weak Chaos: 1D DKG and 1D DDNLS

1D
DKG



1D
DDNLS

Average over 100 realizations [Senyange, Many Manda & S., PRE (2018)]

Block excitation (L=37 sites) $H_{1K}=0.37$, W=3

Single site excitation $H_{1K}=0.4$, W=4

Block excitation (L=21 sites) $H_{1K}=0.21$, W=4

Block excitation (L=13 sites) $H_{1K}=0.26$, W=5

Block excitation (L=21 sites) $\beta=0.04$, W=4

Single site excitation $\beta=1$, W=4

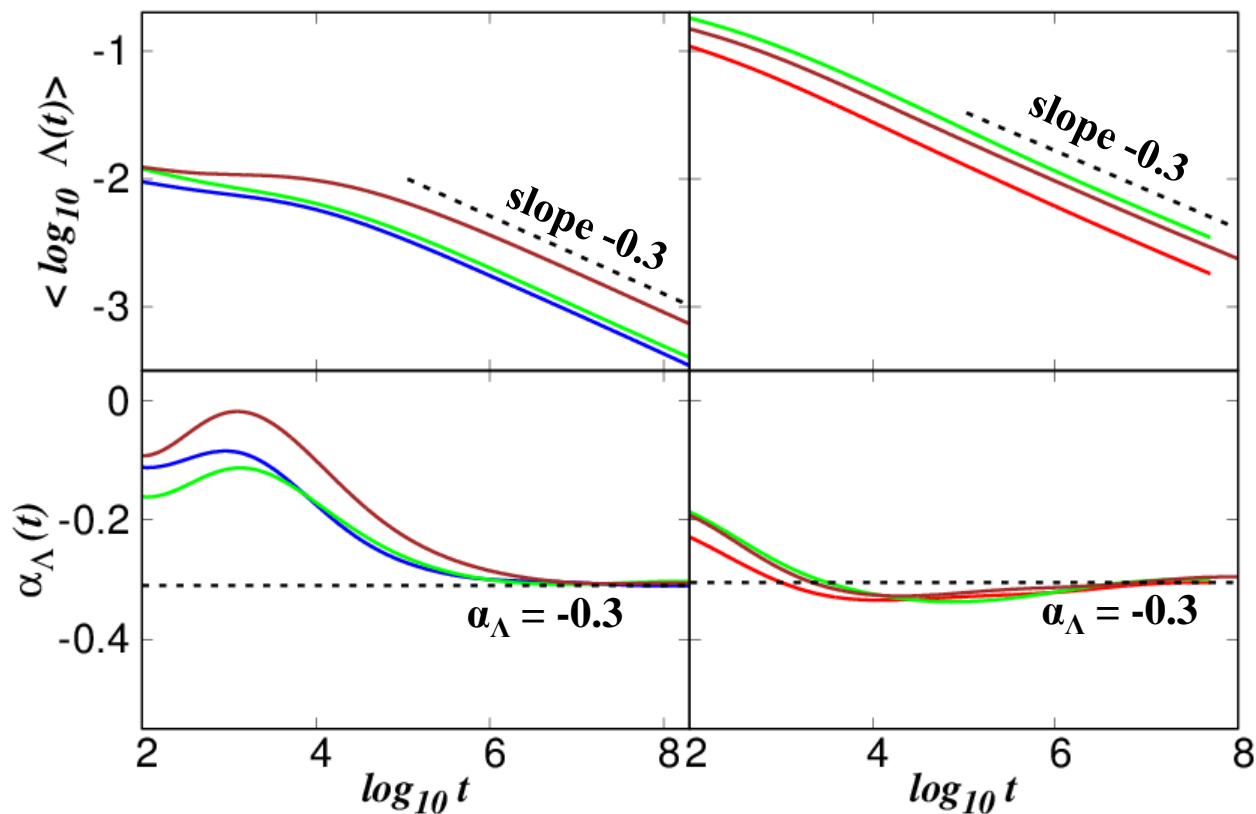
Single site excitation $\beta=0.6$, W=3

Block excitation (L=21 sites) $\beta=0.03$, W=3

1D DKG model also studied in S. et al., PRL (2013)

Strong Chaos: 1D DKG and 1D DDNLS

1D
DKG

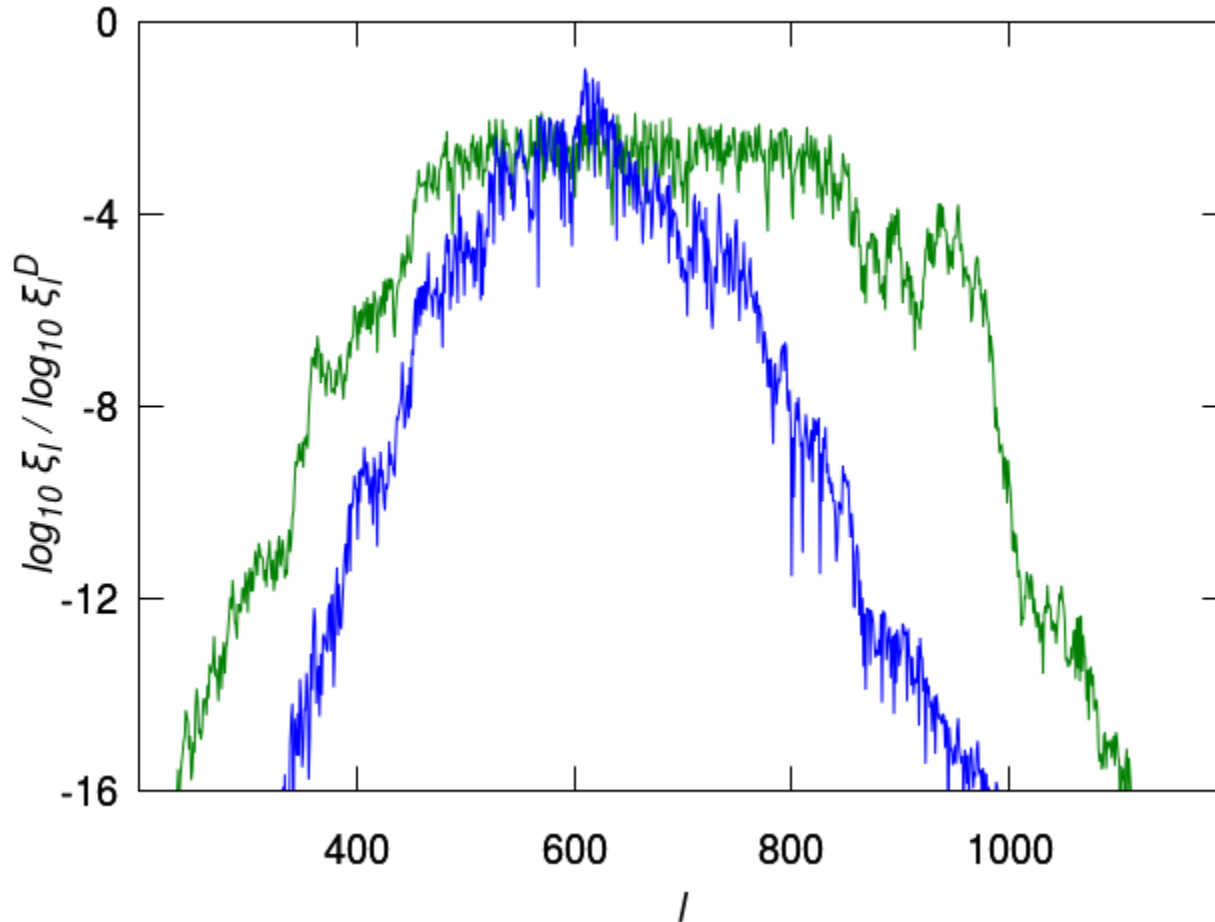


1D
DDNLS

Average over 100 realizations [Senyange, Many Manda & S., PRE (2018)]

Block excitation (L=83 sites) $H_{1K}=0.83$, $W=2$ Block excitation (L=21 sites) $\beta=0.62$, $W=3.5$
 Block excitation (L=37 sites) $H_{1K}=0.37$, $W=3$ Block excitation (L=21 sites) $\beta=0.5$, $W=3$
 Block excitation (L=83 sites) $H_{1K}=0.83$, $W=3$ Block excitation (L=21 sites) $\beta=0.72$, $W=3.5$

Deviation Vector Distributions (DVDs)



Energy
DVD

1D DKG
weak chaos
L=37 sites,
H_{1K}=0.37,
W=3

Deviation vector:

$$\mathbf{v}(t) = (\delta u_1(t), \delta u_2(t), \dots, \delta u_N(t), \delta p_1(t), \delta p_2(t), \dots, \delta p_N(t))$$

$$\text{DVD: } \xi_l^D = \frac{\delta u_l^2 + \delta p_l^2}{\sum_l (\delta u_l^2 + \delta p_l^2)}$$

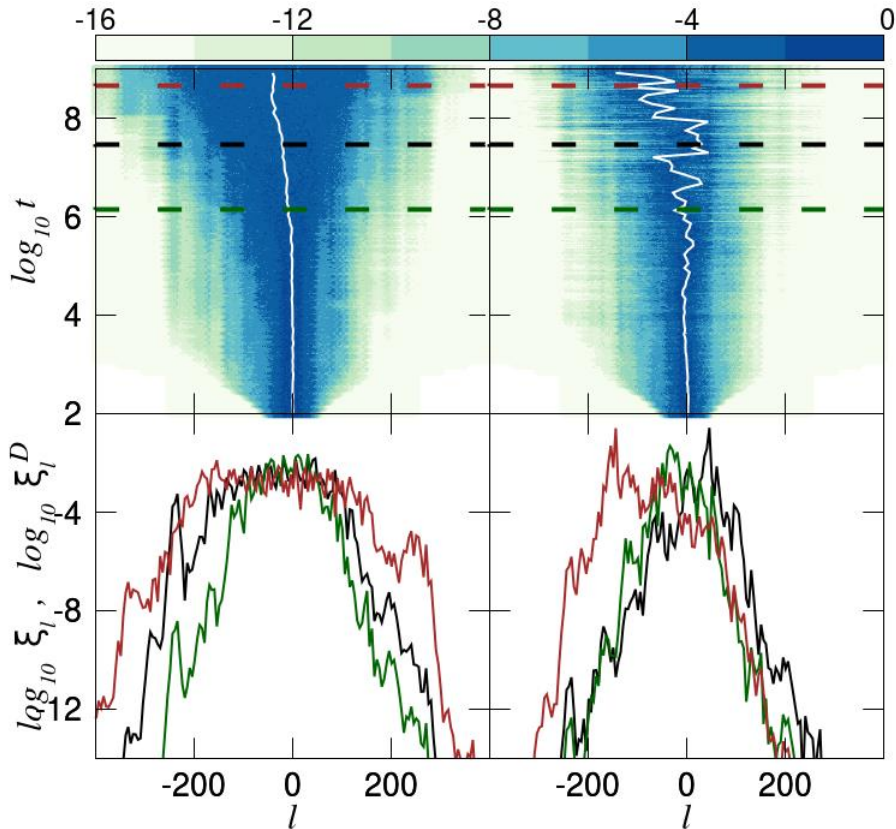
DVDs: Weak and Strong Chaos

Weak chaos (1D DKG)

Strong chaos (1D DKG)

Energy

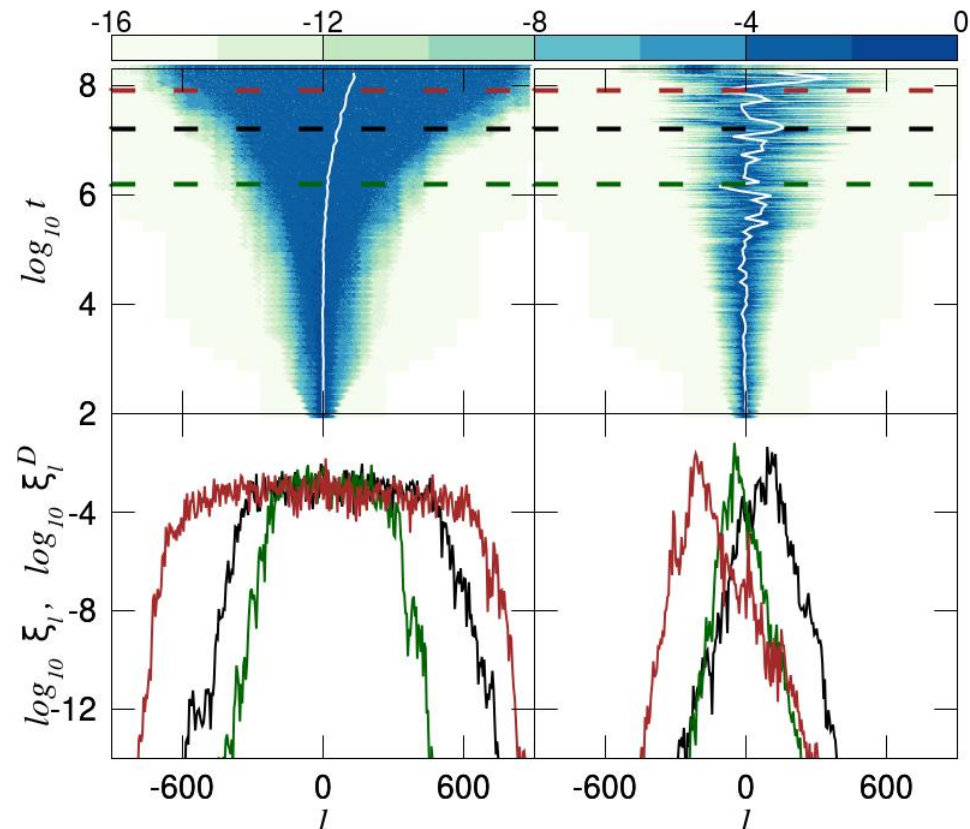
DVD



$W=3, L=37, H=0.37$

Energy

DVD



$W=3, L=83, H=8.3$

Chaotic hot spots meander through the system, supporting the homogeneity of chaos inside the wave packet.

Frequency Map Analysis (FMA)

Compute the **fundamental frequencies**, f_1 and f_2 , of an observable related to the evolution of an orbit in **two successive time windows** of the same length, and check **whether or not these frequencies change in time** [Laskar, Icarus (1990) – Laskar et al., Physica D (1992) – Laskar, Physica D (1993) – Robutel & Laskar, Icarus (2000)].

Regular motion: The computed frequencies do not vary in time

Chaotic motion: The computed frequencies vary in time

For every lattice site l we compute the fundamental frequencies f_{1l} and f_{2l} for time windows of length $T = 6 \cdot 10^5$ time units and evaluate the **relative change of these two frequencies**:

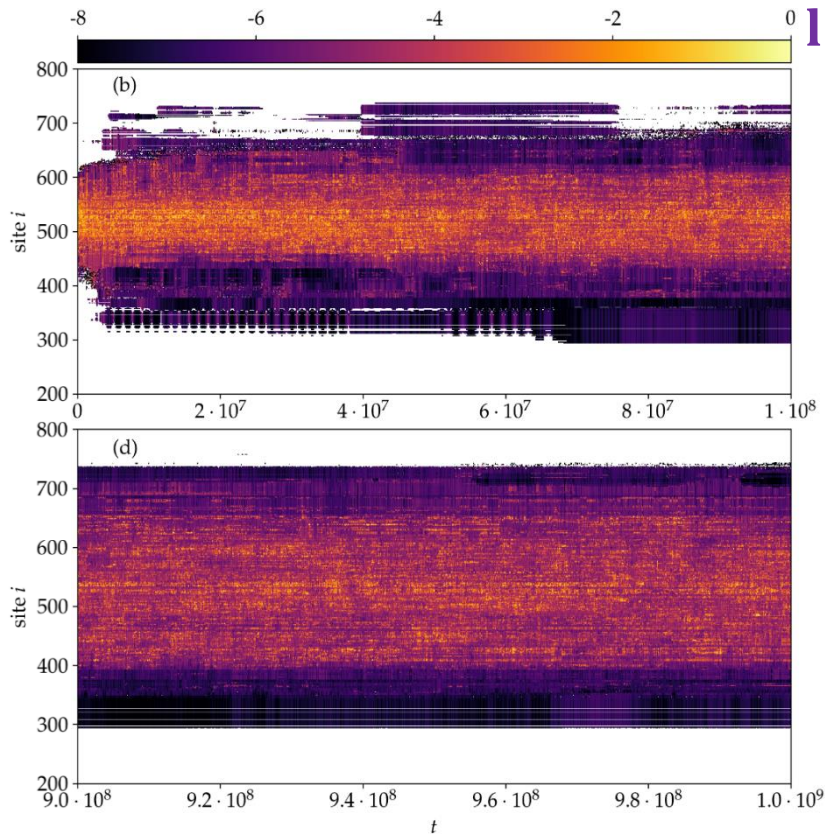
$$D_l = \left| \frac{f_{2l} - f_{1l}}{f_{1l}} \right|$$

Regular motion: small D_l values

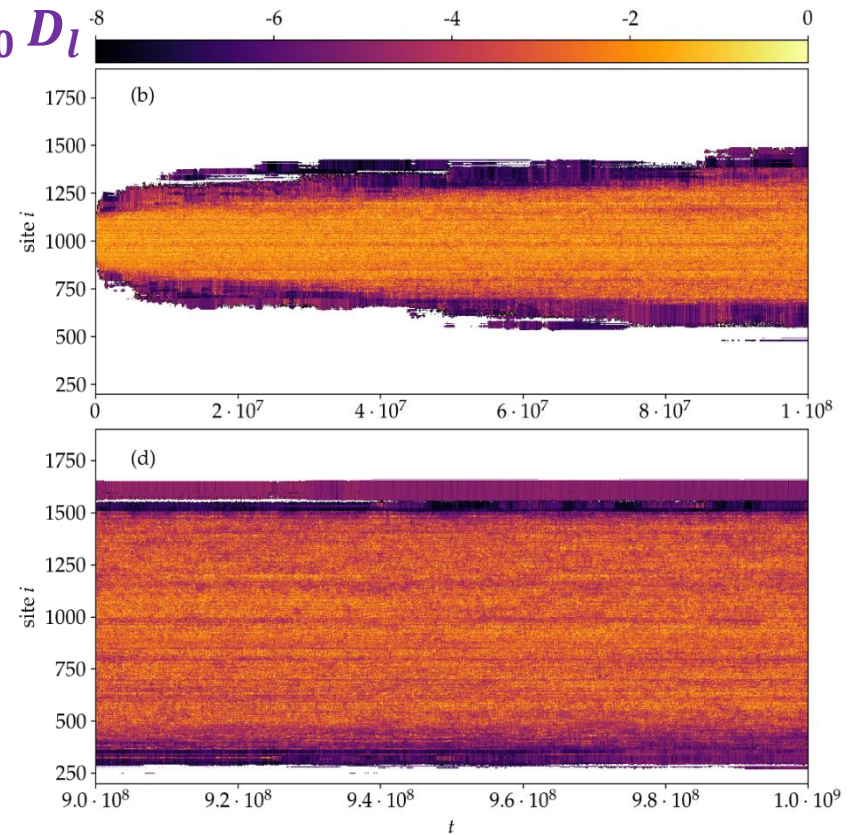
Chaotic motion: large D_l values

FMA: Weak and Strong Chaos

Weak chaos
 $L=1, H=0.4, W=4, N=999$



Strong chaos
 $L=21, H=4.2, W=4, N=3499$

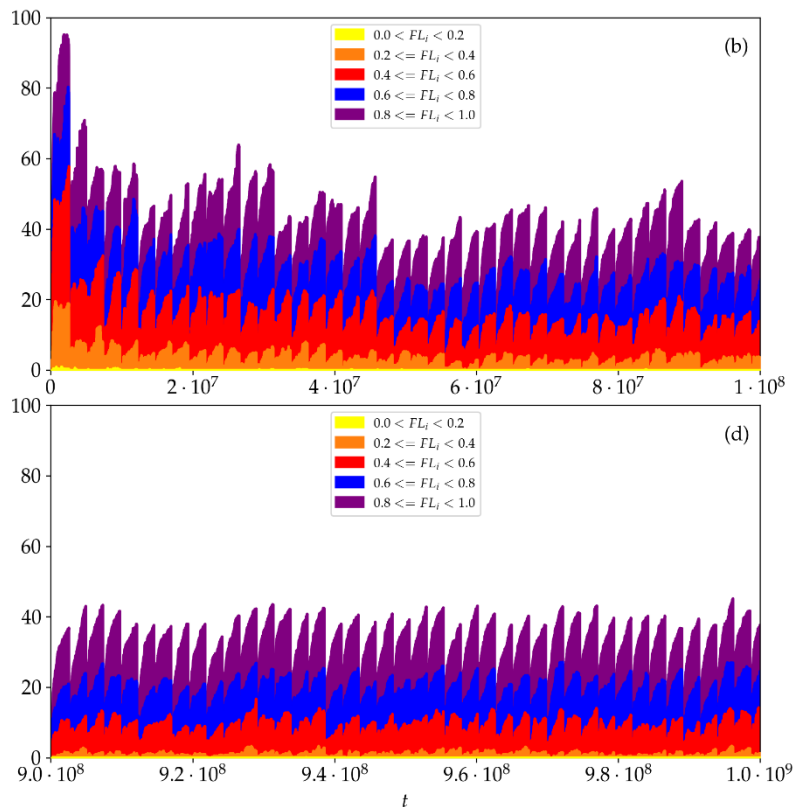


Chaotic behavior appears at the central regions of the wave packet, where the energy density is relatively large. The chaotic component of the wave packet **is more extended in the strong chaos case** [S. et al., IJBC (2022)]

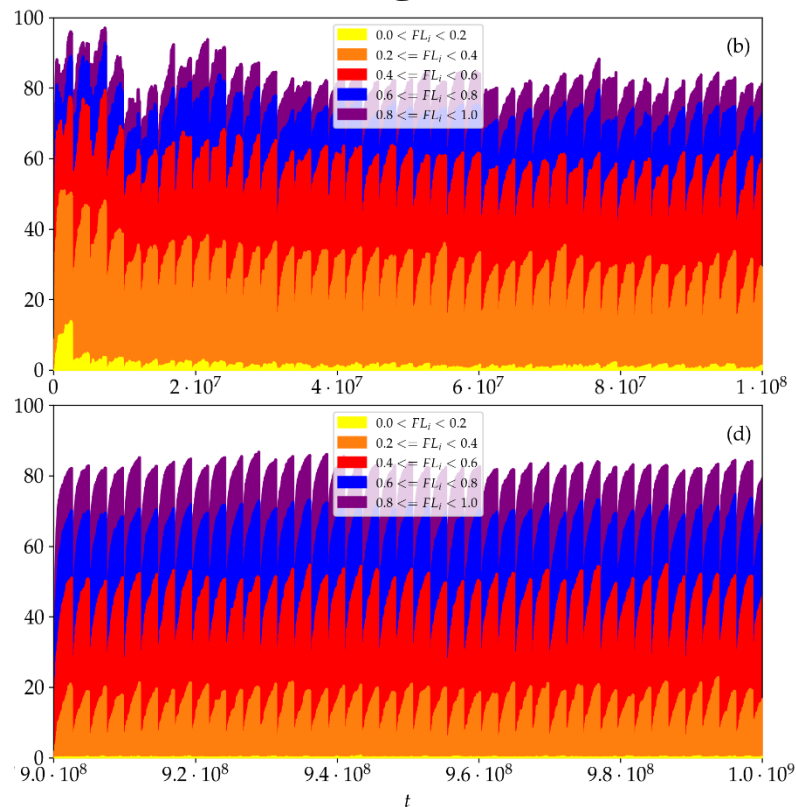
Frequency Locking (FL)

Accumulated percentages P_{FL} of sites with values in a particular FL range

Weak chaos



Strong chaos



The fraction of **sites behaving chaotically** is much larger in the strong chaos regime.

The percentage of **strongly chaotic sites (having $FL_i < 0.4$)** is about 5 times larger for strong chaos.

For **both spreading regimes, the fraction of highly chaotic oscillators ($FL_i < 0.4$) decreases in time**, although the percentage of chaotic sites remains practically constant.

The Generalized Alignment Index (GALI)

In the case of an N degree of freedom Hamiltonian system we follow the evolution of k deviation vectors with $2 \leq k \leq 2N$, and define [S. et al., Physica D, (2007)] the Generalized Alignment Index (GALI) of order k :

$$GALI_k(t) = \|\hat{v}_1(t) \wedge \hat{v}_2(t) \wedge \dots \wedge \hat{v}_k(t)\|$$

where $\hat{v}_1(t) = \frac{v_1(t)}{\|v_1(t)\|}$.

Chaotic motion: $GALI_k(t) \propto e^{-[(\lambda_1 - \lambda_2) + (\lambda_1 - \lambda_3) + \dots + (\lambda_1 - \lambda_k)]t}$
with $\lambda_1, \lambda_2, \dots, \lambda_k$ being the first k largest Lyapunov exponents.

Regular motion: When the motion occurs on an N -dimensional torus [S. et al., Eur. Phys. J. Sp. Top. (2008)]:

$$GALI_k(t) \propto \text{constant, if } 2 \leq k \leq N$$

Here we consider $GALI_2$ ($k=2$) which is equivalent to the **Smaller Alignment Index (SALI)** [S, J. Phys A (2001)].

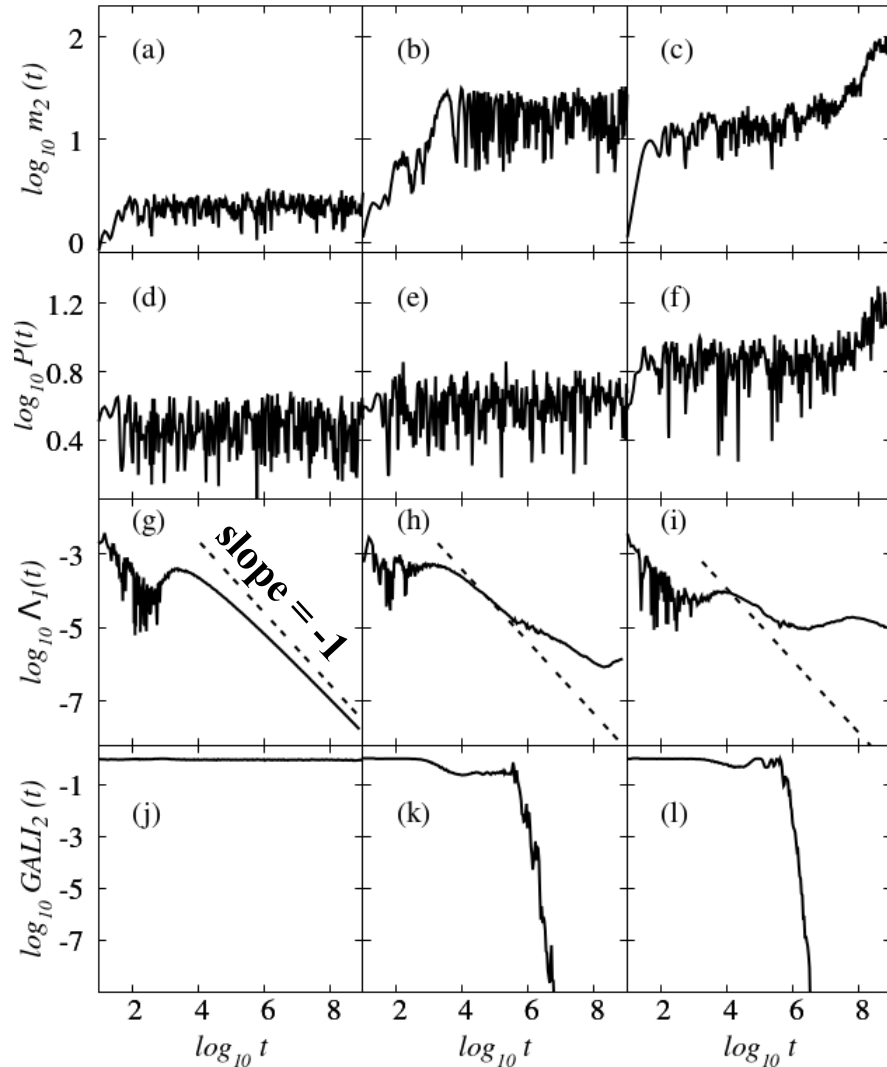
Regular vs. chaotic (localized or spreading) motion

Different disorder realizations can exhibit different behaviors.

Regular
motion

Localized
chaos

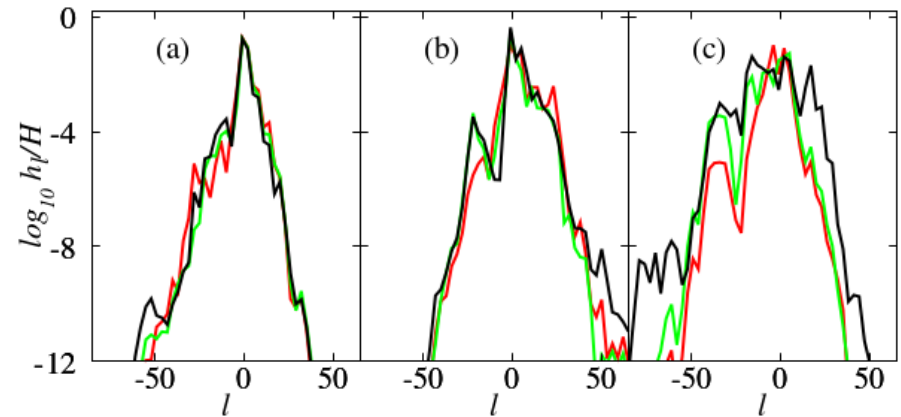
Spreading
chaos



Regular
motion

Localized
chaos

Spreading
chaos



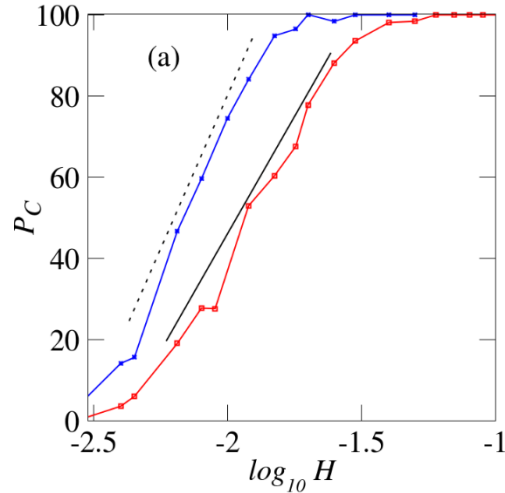
$$t = 10^5, 10^7, 10^9$$

Single site excitations, $L=1$, for
 $W=6$, $H=0.02$ [Senyange & S.,
Physica D (2022)].

The $GALL_2$ can identify chaos
much more clearly than the MLE.

Decreasing nonlinearity

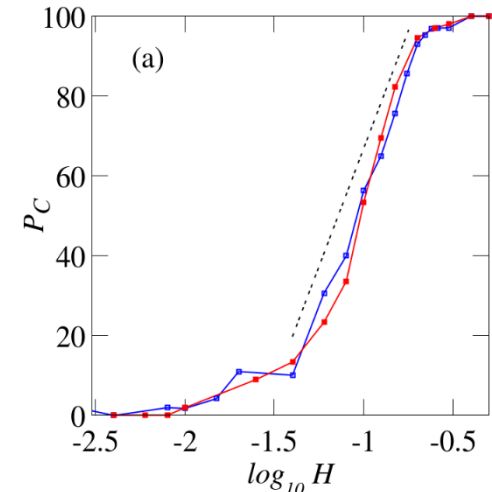
Single site excitations



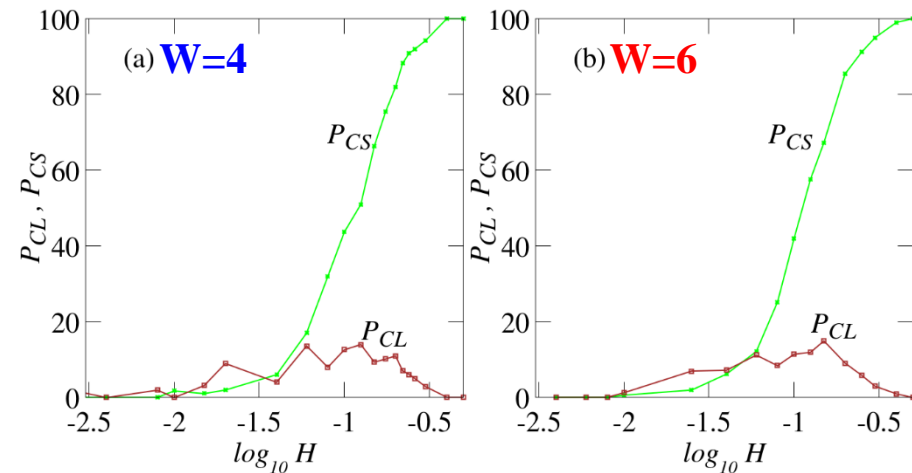
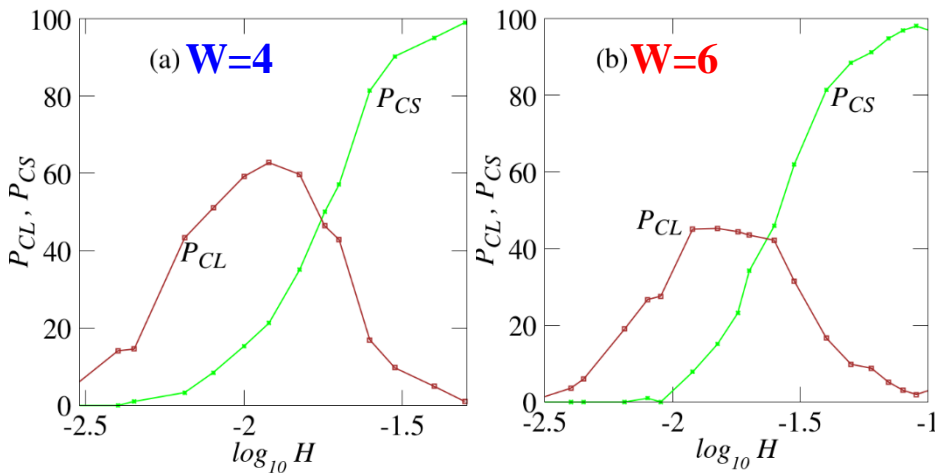
P_C : % of chaotic orbits

$W=4$, $W=6$

Single mode excitations



P_{CL} : % of localized chaos P_{CS} : % of spreading chaos



Energy thresholds for transition to regular motion and to spreading chaos are lower for single site excitations which permit mode interactions [Senyange & S., Physica D (2022)].

The 2D DKG model

$$H_{2K} = \sum_{l,m} \left\{ \frac{p_{l,m}^2}{2} + \frac{\tilde{\varepsilon}_{l,m}}{2} u_{l,m}^2 + \frac{u_{l,m}^4}{4} + \frac{1}{2W} \left[(u_{l,m+1} - u_{l,m})^2 + (u_{l+1,m} - u_{l,m})^2 \right] \right\}$$

Again we have **fixed boundary conditions** and $\tilde{\varepsilon}_{l,m}$ are chosen uniformly in $\left[\frac{1}{2}, \frac{3}{2} \right]$.

The 2D DDNLS system

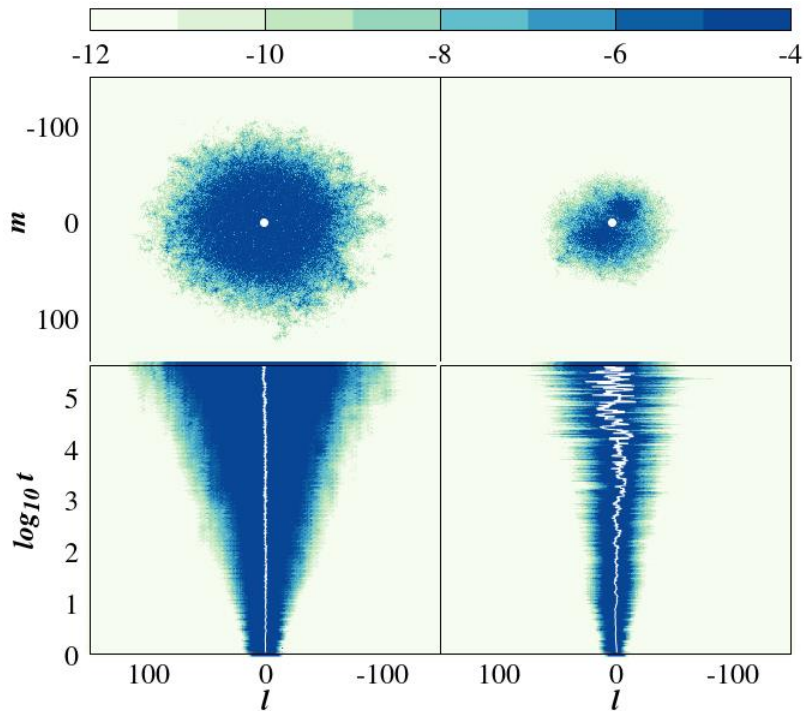
$$H_{2D} = \sum_{l,m} \left\{ \frac{\varepsilon_{l,m}}{2} (u_{l,m}^2 + p_{l,m}^2) + \frac{\beta}{8} (u_{l,m}^2 + p_{l,m}^2)^2 - (u_{l,m+1}u_{l,m} + u_{l+1,m}u_{l,m} + p_{l,m+1}p_{l,m} + p_{l+1,m}p_{l,m}) \right\}$$

Again ε_l are chosen uniformly from $\left[-\frac{W}{2}, \frac{W}{2} \right]$ and β is the nonlinear parameter.

Conserved quantities: The energy H_{2D} and the norm $S = \sum_{l,m} \frac{u_{l,m}^2 + p_{l,m}^2}{2}$

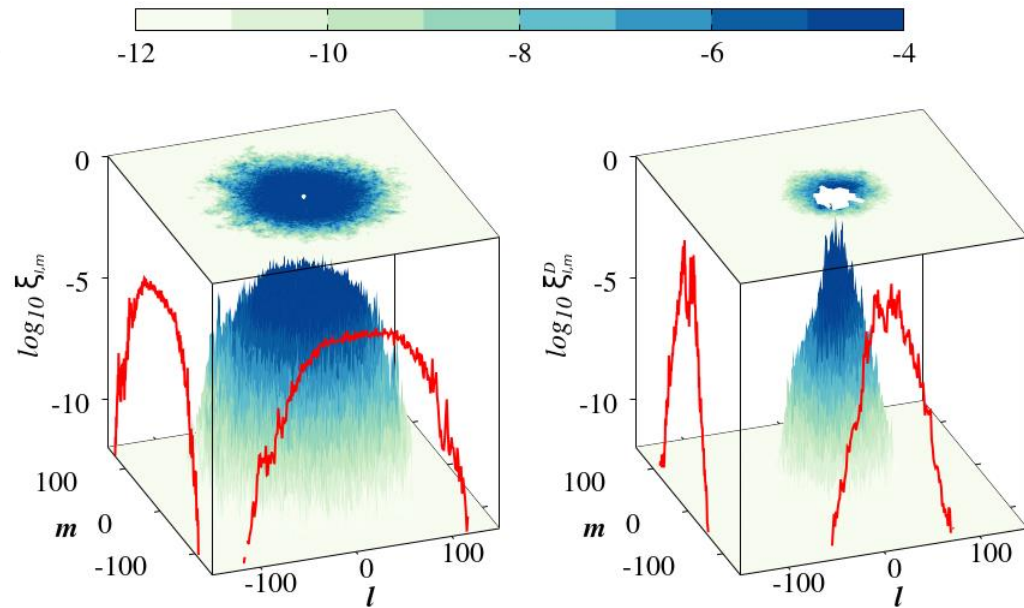
2D: Deviation Vector Distributions (DVDs)

2D DDNLS: strong chaos
 $L=15, W=12, \beta=0.425, s_{l,m}=1, H_{2D}=1.32$



Norm

DVD



Norm

DVD

Dimension-independent scaling between chaoticity and spreading

Second moment: Theoretical predictions verified by numerical computations

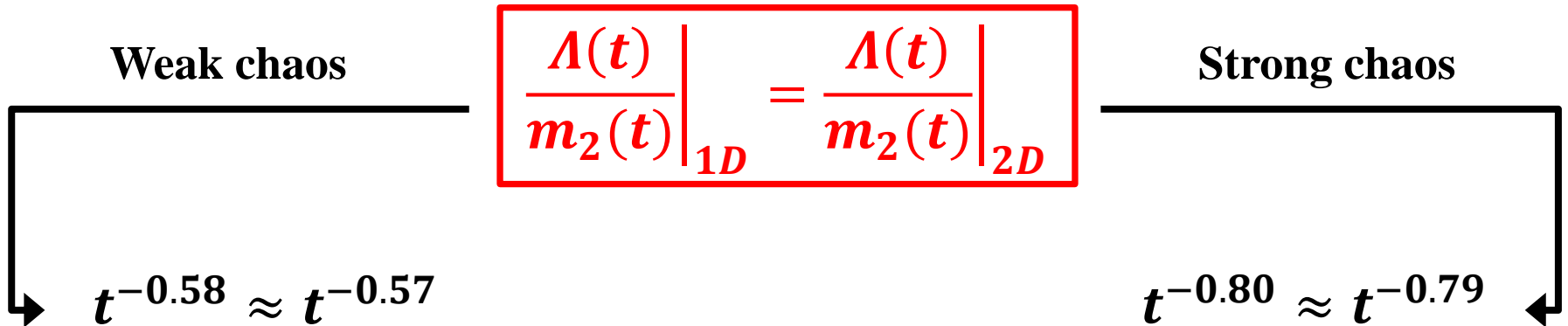
$$m_2 \propto t^{a_m}$$

a_m	Weak	Strong
1D	1/3	1/2
2D	1/5	1/3

a_Λ	Weak	Strong
1D	-0.25	-0.30
2D	-0.37	-0.46

$\Lambda \propto t^{a_\Lambda}$ Finite time mLCE: Numerical computations

For 1D and 2D systems there exists a uniform *scaling between the wave packet's spreading and its degree of chaoticity* indicating that nonlinear interactions of the same nature are responsible for the chaotic wave-packet spreading in both cases.



References

- Flach, Krimer, S. (2009) PRL, 102, 024101
- S., Krimer, Komineas, Flach (2009) PRE, 79, 056211
- S., Flach (2010) PRE, 82, 016208
- Lapyteva, Bodyfelt, Krimer, S., Flach (2010) EPL, 91, 30001
- Bodyfelt, Lapyteva, S., Krimer, Flach (2011) PRE, 84, 016205
- Bodyfelt, Lapyteva, Gligoric, S., Krimer, Flach (2011) IJBC, 21, 2107
- S., Gkolas, Flach (2013) PRL, 111, 064101
- Tieleman, S., Lazarides (2014) EPL, 105, 20001
- Antonopoulos, Bountis, S., Drossos (2014) Chaos, 24, 024405
- Antonopoulos, S., Bountis, Flach (2017) Chaos Sol. Fract., 104, 129
- Senyange, Many Manda, S. (2018) PRE, 98, 052229
- Many Manda, Senyange, S. (2020) PRE, 101, 032206
- Senyange, S. (2022) Physica D, 432, 133154
- S., Gerlach, Flach (2022) Int. J. Bifurc. Chaos, 32, 2250074

Dynamics of disordered lattices

-
- S., Gerlach (2010) PRE, 82, 036704
 - Gerlach, S. (2011) Discr. Cont. Dyn. Sys.-Supp., 2011, 475
 - Gerlach, Eggl, S. (2012) IJBC, 22, 1250216
 - S., Gerlach, Bodyfelt, Papamikos, Eggl (2014) Phys. Lett. A, 378, 1809
 - Gerlach, Meichsner, S. (2016) Eur. Phys. J. Sp. Top., 225, 1103
 - Senyange, S. (2018) Eur. Phys. J. Sp. Top., 227, 625
 - Danieli, Many Manda, Mithun, S. (2019) MinE, 1, 447

*Numerical integration of
multidimensional Hamiltonian systems*

-
- S. (2001) J. Phys. A, 34, 10029
 - S., Bountis, Antonopoulos (2007) Physica D, 231, 30
 - S., Bountis, Antonopoulos (2008) Eur. Phys. J. Sp. Top., 165, 5
 - S. (2010) Lect. Notes Phys., 790, 63
 - S., Manos (2016) Lect. Notes Phys., 915, 129

Chaos detection techniques